A Numerical Investigation on the Collapse of the Champlain Towers South in Florida

Daigoro Isobe[1,*], Junnan Zhu[2], and Janine Pardee[3]
[1]Division of Engineering Mechanics and Energy, University of Tsukuba, Tsukuba-shi, Ibaraki, Japan
[2]Graduate School, University of Tsukuba, Tsukuba-shi, Ibaraki, Japan
[3]Orbit City Engineering LLC, Florida, USA
Email: isobe@kz.tsukuba.ac.jp (D.I.); zhu.junnan.su@alumni.tsukuba.ac.jp(J.Z.); janinepardee@yahoo.com(J.P.)
*Corresponding author

Abstract—**In this study, the Champlain Towers South building collapse in Florida allegedly caused by a deck collapse was examined through the finite element analysis based on the existing hypotheses and investigation. The Adaptively Shifted Integration (ASI) – Gauss code was applied for the numerical analysis. In addition, the member strength failure algorithm of RC components was modified, and the flat-plate structure was introduced into the numerical model of the building. According to the analyses, the building did not collapse when the pool deck beams connecting to the columns of the 1st-floor interior, so-called key columns, were removed by the collapse of the pool deck. When the model was revised to include deterioration of concrete slab and corrosion of rebars, and then triggered by the removal of columns in the underground parking garage, the middle section of the buildings reached a total collapse. This supports the latest collapse theories, which cite punching shear failure at pool deck columns as the initiating event.**

***Keywords*—collapse analysis, flat-plate structure, RC building, deterioration, corrosion, ASI–Gauss code**

I. Introduction

The middle and eastern sections of Champlain Towers South in Florida (Fig. 1), USA, a 13-story condominium built in 1981, collapsed without warning at approximately 1:25 a.m. on June 24, 2021. According to the surveillance video [1], the collapses of the middle section and the following eastern section only lasted for 12 seconds (Fig. 2). At least half of the 136 units in the building had collapsed (Fig. 3), and all of them were characterized by the fact that they collapsed instantly after it began to collapse. The U.S. National Institute of Standards and Technology (NIST) investigated the collapse the following day, June 25, and a total of 98 deaths were confirmed as of July 22, 2021 [2]. It is currently believed by many that the direct cause was the additional concrete, sand, and pavers placed on the surface layer of the pool deck located in the southeast area of the building in 1996. This increased its weight, causing the deck to finally cave in as punching shear gradually progressed between it and the columns in the basement [3]. The collapse of the deck reduced the buckling capacity of the first-floor columns, or the failure of the connection dragged the columns into failure, leading to the progressive collapse of two-thirds of the building. Others believe that the main causes of the collapse were water infiltration and the deterioration of the reinforced concrete of the parking lot beneath the housing units due to corrosion of the rebar. Florida is a regular hurricane zone, and as buildings are exposed to saltwater, deterioration is likely to progress. Also, the possibility that the direct trigger of the collapse was a collision of a vehicle with a column in the basement garage cannot yet be ruled out.

Fig. 1. Champlain Towers South Condominium.

In October 2018, Morabito *et al.* [4] reported to residents that they found "significant structural damage" to pool decks, adjacent driveways, and planters where corrosion had been caused by water penetration. The report noted that various cracks and spalling of concrete were also found in the columns, beams, walls, and entrance deck of the underground parking garage. The most severe deterioration was found in the underground parking garage and the ground deck. Cracks and spalling of concrete were found in the parking lot columns and spalling with exposed steel rebar was found at topside of the garage deck. Also, punching-related distress was found slowly progressing in the concrete around planters on the pool deck. Furthermore, the penthouse on the 13th floor did not exist at the start of construction and was added after construction started, apparently without re-design of the lower structure. This

Manuscript received May 25, 2024; revised August 22, 2024; accepted September 4, 2024; published January 20, 2025.

Photographs from Figs. 8 to 13: © Janine Pardee

doi: 10.18178/ijscer.14.1.1-9

would have increased the risk of exceeding the load-bearing capacity of the condominium.

(a) 1 s from collapse initiation (b) 3 s from collapse initiation

(c) 5 s from collapse initiation (d) 12 s from collapse initiation

Fig. 2. Collapse sequence of the Champlain Towers South [1].

In addition, 90% of the high-rise buildings on Florida's east coast are flat-plate structures, and Champlain Towers South was one of them. Flat-plate structures are slab-tied to columns without beams, and this structure is known to be very sensitive to punching shear. Another Florida condominium with a similar flat-plate design collapsed during construction in 1981. NIST also investigated this collapse of Harbour Cay in Cocoa Beach, and the cause was described as punching shear failures [5].

Fig. 3. Collapsed site of the Champlain Towers South.

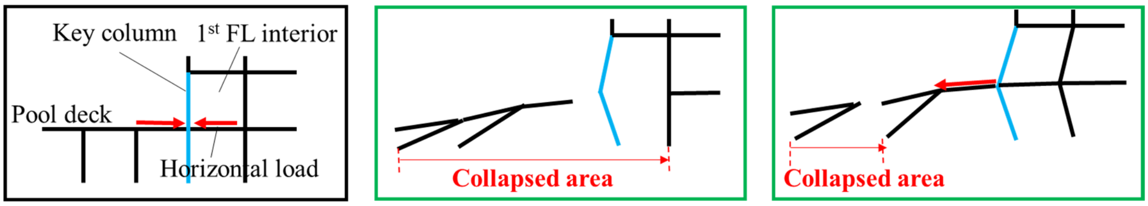

(a) State before collapse (b) First hypothesis by Mosalam *et al.* (c) Second hypothesis by Porter *et al.*

Fig. 4. Hypotheses of the building collapse.

Two hypotheses presented in the Washington Post [6] suggests that the collapse of the pool deck into the underground parking garage may have weakened the key columns and caused the widespread collapse. The light blue member shown in Fig. 4(a) is a key column that is critical to the support of the building. The red arrows in the figure indicate the horizontal loads acting on the column. The left side of the key column represents the pool deck connected to the building, and the right side represents the 1st-floor interior. An illustration explaining the first hypothesis by Mosalam *et al.* is shown in Fig. 4(b). It states that the collapse of the pool deck extended beyond the key columns, causing the columns to buckle due to overloading caused by the loss of horizontal support on the deck side. In this study, we call this Hypothesis 1. An illustration explaining the second hypothesis by Porter *et al.* is shown in Fig. 4(c). It states that the collapse of the pool deck was not so extensive that the key columns were pulled by the surrounding deck beams, causing the key columns to collapse together with the pool deck beams. We call this Hypothesis 2.

In this study, verification analyses were conducted to determine whether the key columns would reach the buckling load and begin to collapse under Hypotheses 1 and 2 explained above. The failure of the connection joints between the pool deck beams and the columns on the 1st floor of the building due to the tension applied from the pool deck was not considered. On the other hand, analyses were also conducted assuming the loss of the columns in the underground parking garage as the trigger for collapse, with simple consideration of the deterioration of the steel bars and concrete.

At the time this study was conducted, some theories and information had not emerged. Observers of the site and the collapse photos have posited that several widespread construction flaws can be observed. These hypothetical construction defects could not be quantified for this analysis. More recently, Wiss, Janney, Elstner Associates, Inc. (WJE) [7] conducted an engineering study for the condominium association, with significant new information and theories of the failure. These hypotheses could not be examined in time for this study.

II. Numerical Framework

In this study, the ASI-Gauss code [8] was employed to simulate the collapse behavior of the building. For problems with strong nonlinear behavior, such as collapse analysis, high computational efficiency and reduced solution time can be achieved using this code. This code has been utilized in various fields, such as impact loading [9], progressive collapse [10, 11], seismic collapse [12], and demolition [13, 14], owing to its numerous advantages and flexibility.

The main idea applied in the ASI-Gauss code is to shift the numerical integration point to an appropriate position on a linear Timoshenko beam element when a plastic section is determined to be formed. When the plastic hinge is later unloaded, the numerical integration point is shifted back to its initial position to accurately capture the elastic unloading behavior. The relationship between the locations of the numerical integration point and the plastic hinge used in the shifting procedure is obtained by comparing the strain energy approximation of the finite element beam model and the rigid body–spring model (RBSM). The RBSM consists of two rigid bars connected by rotational and shear springs that simulate the plastic hinge by reducing the stiffness of the springs. The yield condition used in this code is expressed as follows [8].

$$f = \left(\frac{M_x}{M_{x0}}\right)^2 + \left(\frac{M_y}{M_{y0}}\right)^2 + \left(\frac{N}{N_0}\right)^2 - 1 \equiv f_y - 1 = 0, \quad (1)$$

where f_y is the yield function, and M_x, M_y, and N are the bending moments around the x-axis, y-axis, and axial forces, respectively. The terms with subscript 0 are values that result in a fully plastic section in an element if they act on the cross-section independently.

Furthermore, the ASI-Gauss code can reduce the inaccuracy arising from the evaluation of the low-order displacement function of the beam element in the elastic range which uses one-point integration. In this code, two consecutive elements are considered subsets of a member. The two integration points in the elements are placed at locations, such that the stress evaluation points in the elastic range coincide with the Gaussian integration points of the member. The stresses and strains in the elastic range are evaluated at the two integration points, while one-point integration is performed on an element. Thus, the appropriate elastoplastic behavior of a member can be attained using a minimum number of elements, thus reducing memory use without sacrificing numerical accuracy.

A degrading trilinear model with viscous damping [15, 16] was used for the constitutive equation of the reinforced concrete members. The failure strength of the RC members was determined by evaluating the shear strains and tensional normal strain for the elements that approached the bending yield strength or ultimate shear strength. The following equations were used to determine the member strength failure [8]:

$$\left|\frac{\gamma_{xz}}{\gamma_{xz0}}\right| - 1 \geq 0 \ or \ \left|\frac{\gamma_{yz}}{\gamma_{yz0}}\right| - 1 \geq 0 \ or \ \left(\frac{\varepsilon_z}{\varepsilon_{z0}}\right) - 1 \geq 0, \quad (2)$$

where γ_{xz}, γ_{yz} and ε_z are the shear strains for the x- and y-axes and the axial tensile strain, respectively. The terms with subscript 0 are the critical values of these strains. A variation in the critical values may affect the results in detail; thus, these values should be carefully selected and validated. In this study, the critical strains for the member strength failure were selected based on the evaluation results of the anti-seismic performance of RC pillars with high-strength rebars [17]. The actual values used in the analyses are presented in the next section.

In this code, the contact between objects is determined by first evaluating the geometric relations between the four nodes constituting two elements in the potential contact. The shortest distance between these two elements is evaluated, and the final contact is determined by examining the angles between the assumed contact point and nodes. Once these two elements are determined to be in contact, they are bound by four gap elements between the nodes. The gap elements are assumed to have the same physical and material properties as those of the nearby elements. These are automatically eliminated when the mean value of the deformation of the four gap elements is reduced to a specified ratio.

The simplifications of the algorithms matched the simplified approximations of structural members using beam elements, and their reliabilities were ensured based on the verification and validation results [13, 18]. Detailed information regarding this technique can be found in [8].

III. Numerical Model and Conditions

A. Numerical Model of the Champlain Towers South

Based on the design drawings of Champlain Towers South [19], the numerical model shown in Fig. 5 was constructed. Its plan, elevation, and side views are shown in Fig. 6. The modeled members were columns, beams, floors, and wind-resistant walls. The flat-plate slabs were modeled using braced beam elements. The total height of the building was 38.506 m. The floor heights of the basement and 1st floor were 3.404 m and 4.166 m, respectively, and the floor heights of the 2nd through 13th floors were 2.692 m each. Gr. 60 with a tensile strength of 420 MPa was used for the main rebars, and Gr. 40 with a tensile strength of 280 MPa was used for the shear rebars. The compressive strengths of the concrete used was 41.4 MPa for the basement through 3rd floors, 34.5 MPa for the 4th through 7th floors, and 27.6 MPa for the 5th through 13th floors. The concrete slabs for the building floors were 203 mm thick, and those for the pool deck floors were 153 mm thick. Floor loads of 6,792 N/m^2 for the building and 3600 N/m^2 for the deck were incorporated into the numerical model by adding to the density of the load-bearing beam and floor members. Wind-resistant walls placed from the basement to the 13th floor were represented by braced beam elements with a thickness of 305 mm. The stiffnesses of both floor members and wall members were set only to allow out-of-plane deformations. The critical strains for strength failure of members [16, 17] were set as shown in Table 1. The natural period of the numerical model constructed under the above conditions was 1.52 s in the X-axis direction (East-West direction) and 0.71 s in the Y-axis direction (North-South direction). The natural period in the Y-axis direction was shorter than that in the X-axis direction because the number of wind-resistant walls in the Y-axis direction was larger than that in the X-axis direction. The total number of elements and nodes in the numerical model was 12,172 and 7350, respectively.

TABLE I. Critical Strain Values for Strength Failure of Members

	Beams and columns	Floors
Axial tensile strain	0.170	0.170
Shear strain for x -axis direction	0.20	0.03
Shear strain for y -axis direction	0.20	0.03

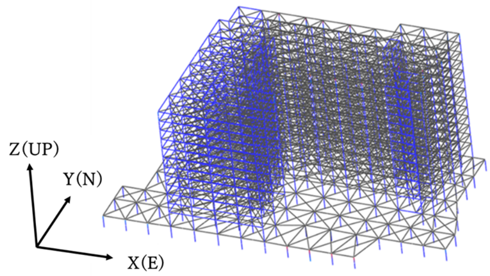

Fig. 5. Finite element model of Champlain Towers South with 1 basement floor and 13 floors above ground.

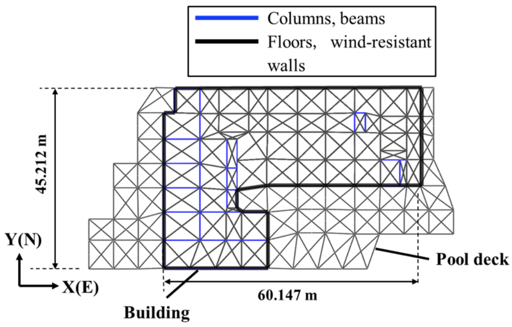

(a) Plan

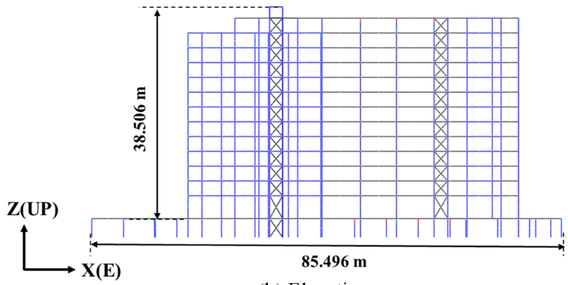

(b) Elevation

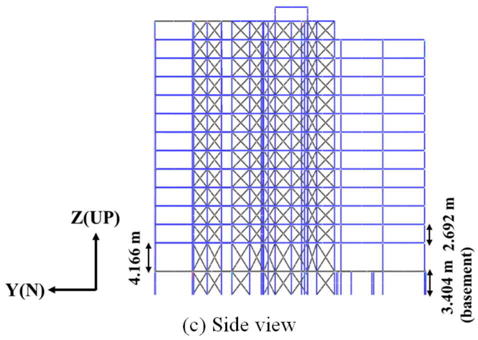

(c) Side view

Fig. 6. Plan, elevation, and side views of the numerical model.

B. Numerical Conditions

To reproduce the conditions in Hypothesis 1, the pool deck collapse was simulated by forcibly disconnecting the members connected to the east, west, and north sides, the members between the key columns, the deck columns, and the floor members inside the building as shown in Fig. 7(a). As for Hypothesis 2, the pool deck collapse was simulated by forcibly disconnecting the members connected to the east and west sides and the deck columns, as shown in Fig. 7(b). The time increment was set to 1 ms, and a total of 3000 steps were computed.

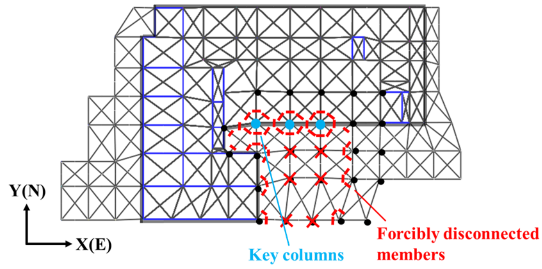

(a) Hypothesis 1

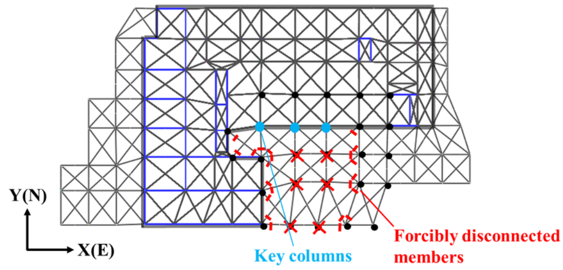

(b) Hypothesis 2

Fig. 7. Numerical conditions based on Hypotheses 1 and 2 [6].

Next, we describe our hypothesis of the collapse process based on the results of the field investigation. The design drawings [19] show that beam members were placed only in the lowest story of the western section of the building, with almost no beam members placed in the middle and eastern sections of the building; the western section was a rigid-frame structure, while the middle and eastern sections were flat-plate structures with relatively low strength. Therefore, as can be seen from the photographs in Figs. 8 and 9, only the west wind-resistant wall remained after the accident, and it was little damaged after the building collapsed. As shown in Figs. 10 and 11, the floor slabs appeared to have been severed at the wind-resistant wall, exposing a meager number of thin and bent rebars. Therefore, it can be inferred that the horizontal rebar in the floor slabs was not entangled with the rebar in vertical members. There was insufficient load transfer from the floor slabs into the columns and wind-resistant walls to form a stable structure. From the images depicted in Fig. 2, it can also be inferred that the initial structural damage began with some of the lower middle columns, and it is possible that the key columns were damaged due to, for example, the failure of the slab-column connections at L13.1 and K13.1 [19], as reported by Fadden [7]. This is supported by Fig. 12, which shows the parking deck columns protruding through the collapsed pool deck slabs, just south of the key columns. The remaining columns may also have had some degree of impairment due to inadequate shear reinforcing, other construction defects, or corrosion. Eventually, the key column-to-slab connections failed, and the remaining weakened columns were no longer strong enough to support the upper loads and buckled, leading to the complete collapse of the middle section. As for the eastern section, the debris piled up after the collapse of the middle section exerted a certain amount of pressure on its lower part, causing damage, which may have triggered its collapse. Fig. 13 supports this scenario, showing that the eastern section “pancaked” down and to the south, then cascaded to the west with increasing displacement.


Fig. 8. Western section remaining after the accident.


Fig. 9. Enlarged photo of a collapsed section.


Fig. 10. Cross-section of a collapsed floor.

Since the rebar at both ends of the floor can be seen to be almost cleanly pulled out as shown in Figs. 10 and 11, the critical value of shear strain of the flat-plate floor members from the ground to the 13th floor, shown in yellow in Fig. 14, was set to 1/1000 to account for the pullout of the rebar at the joint between the wind-resistant wall and the flat-plate floor. The weakening of the concrete and reinforcing bars in the subterranean columns was also considered based on the nearly vertical drop of the middle building seen in Fig. 2. According to Sancheza *et al.* [20], after a certain degree of concrete deterioration, the compressive strength reduces about 35% and the modulus of elasticity about 70% at maximum. Therefore, the compressive strength and modulus of elasticity of the concrete in the basement columns were set to 65% and 30% of their original values, respectively, to follow a worst-case scenario. In addition, the tensile yield stress of the steel bars and shear rebars was set to 1/200 of their original values to account for the deterioration of the rebars and poor workmanship. The columns shown in green in Fig. 14 are the columns with lowered bearing capacity. In the analysis, the damage to the subterranean columns caused by a vehicle impact was assumed by forcibly disconnecting the key columns and the floor members of the deck connected to the key columns, shown in red in the figure.


Fig. 11. Wind-resistant wall of western section left at accident site.


Fig. 12. South end of the uncollapsed western section. This photo is looking west. It can be inferred that the entire pool deck plus two bays of the first level parking slab collapsed in punching shear. The columns of the building did not collapse despite the increased unbraced length. The column labeled for parking space 75 is K-13.1 and the one in front of it is L-13.1. The pool deck collapse is attributed to these two slab-column failures.


Fig. 13. Slabs of the eastern section. This photo is looking north from the pool deck across the debris pile. The roof is at the left, the tan tile is on the 13th story balcony slab, the red tiles on 12th, and so on, with the pink tile at far right the 9th floor balcony. This indicates the eastern section toppled south and then west.

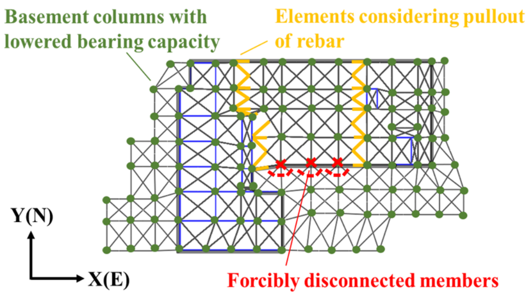

Fig. 14. Numerical conditions based on the hypothesis with deterioration of concrete slabs, corrosion of rebars, and loss of key columns as the main cause.

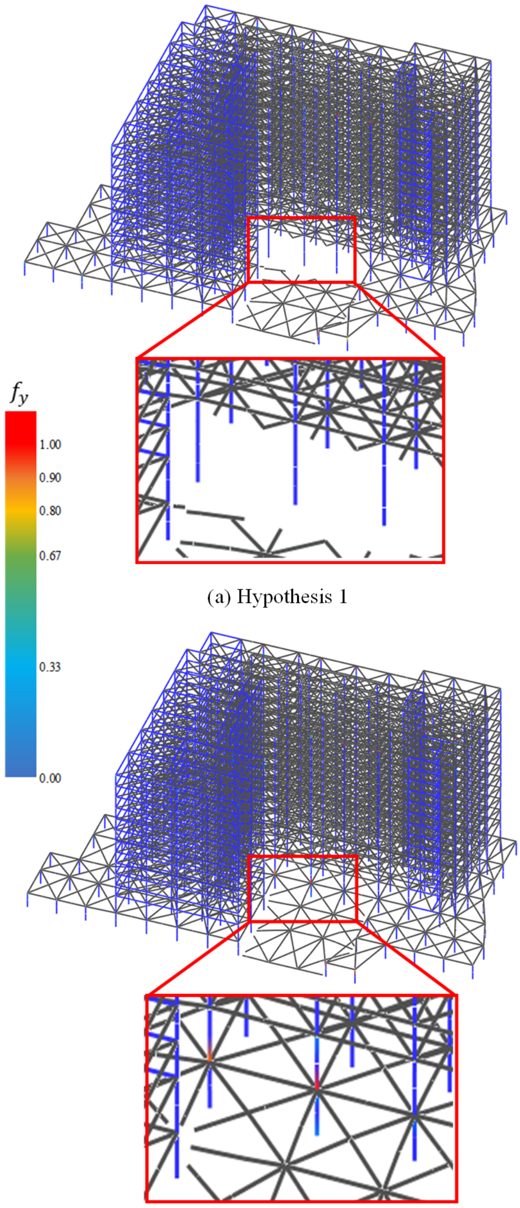

(a) Hypothesis 1

(b) Hypothesis 2

Fig. 15. Numerical results based on the hypotheses with pool deck collapse as the main cause.

IV. Numerical Results

When the extent of pool deck failure exceeded the key columns as in Hypothesis 1, the key columns did not buckle and did not lead to a final collapse state (Fig.15(a)). In the case where the extent of pool deck failure did not exceed the key column as in Hypothesis 2, the key column lead to a final collapse state, but the entire building did not collapse (Fig. 15(b)). These results suggest that other factors may have triggered the collapse of the building. It should be noted here, again, that the analyses for Hypotheses 1 and 2 did not consider the failure of the connection joints between the pool deck beams and the 1st-floor columns, and there is still room for consideration.

Fig. 16 shows the collapse process of the model considering the reduction in bearing capacity of the reinforced concrete, the pullout of the rebar, and the loss of key columns at the start of the analysis (t = 0.0 s). As shown in Fig. 16(a), when the reduction in bearing capacity of the basement columns was considered, the columns were in the final state from the beginning; they are shown in red in the figure. The key column and floor members were fractured at t = 0.005 s. Subsequently, the joints at both ends of the middle section began to fracture under their weight, and the middle section of the building fell. Then, at t = 2.0 s, all the joints at both ends are fractured, as shown in Fig. 16(b). The remaining subterranean columns could no longer withstand the vertical load and the building tilted to the north. The subterranean columns are completely grounded to the floor, as shown in Fig. 16(c), at t = 2.7 s. 5.0 s after the start of the analysis, as shown in Fig. 16(d), the columns in the 7th to 8th floors collapsed in the East-West direction and fell on top of the 6th floor. Then, at t = 8.0 s, the columns in the 6th to 9th floors collapsed and the floors piled up, as shown in Fig. 16(e). The 5th to 7th floors in the eastern section were in contact with the 11th to 13th floors in the middle section and were vibrating slightly. After 15.0 s from the start of the analysis, only the middle section collapsed completely, as shown in Fig. 16(f), and the eastern section did not collapse. Fig. 17 shows an isometric view of the numerical result at t = 15.0 s.

For comparison, a collapse analysis was also performed for a model that did not consider the pullout of steel bars and the reduction in the bearing capacity of reinforced concrete under the same numerical conditions. Although the key columns and floor members were missing from the initial numerical model, the entire model did not collapse at all. From these results, it can be inferred that the middle section did not collapse due to the missing key columns and floor members alone.

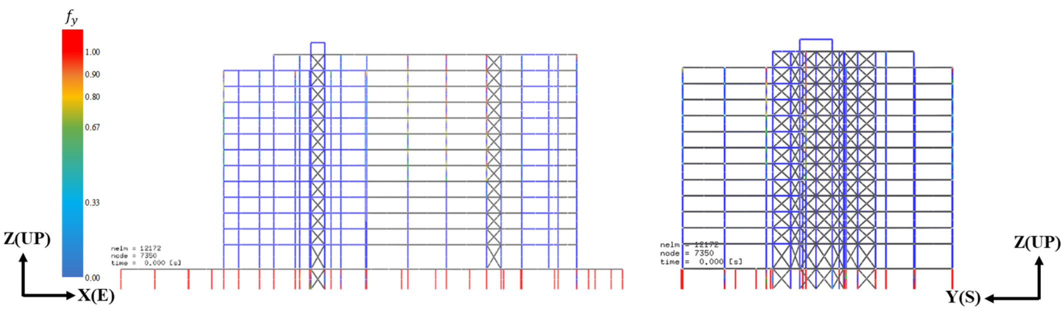

(a) t = 0.0 s

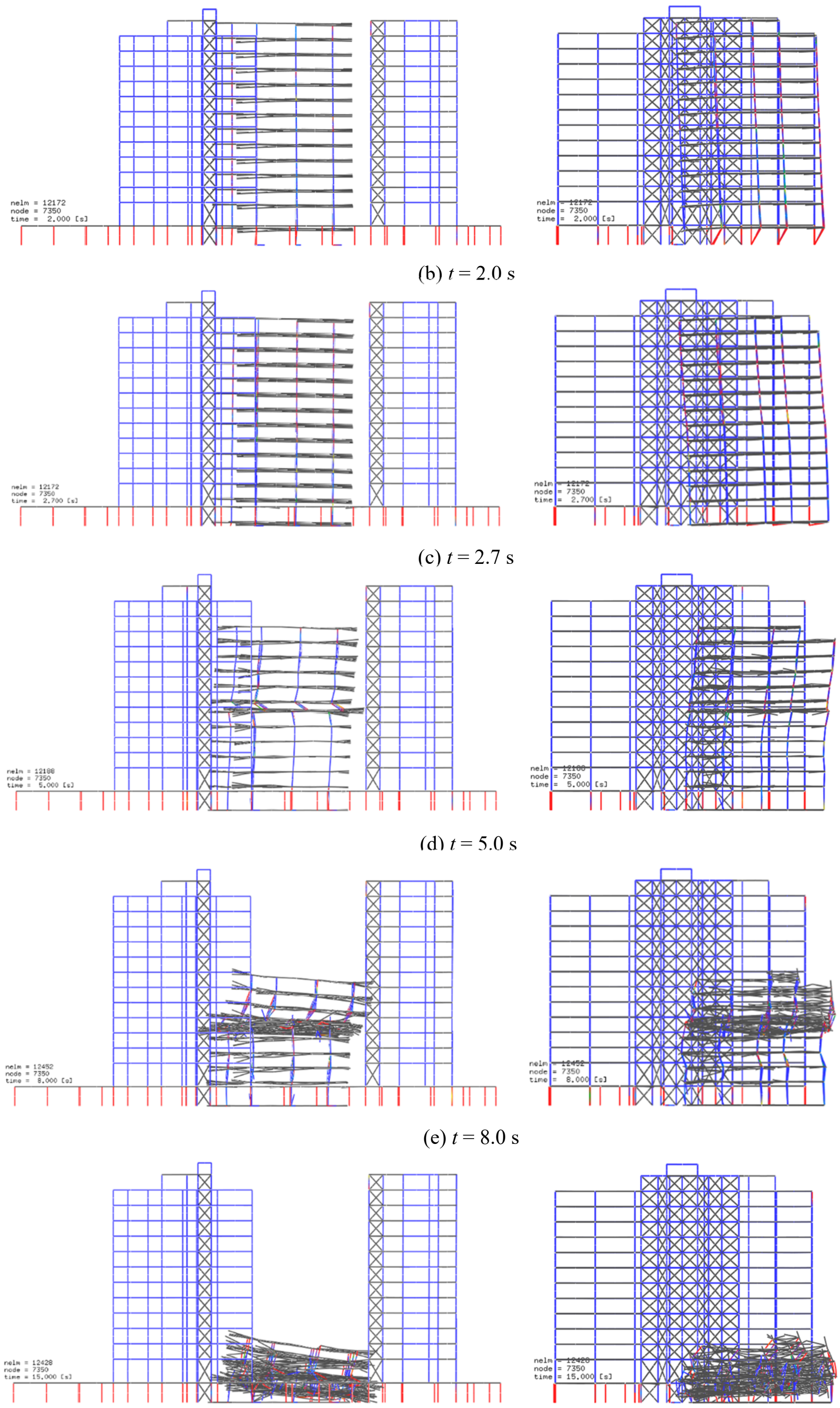

(b) $t = 2.0$ s

(c) $t = 2.7$ s

(d) $t = 5.0$ s

(e) $t = 8.0$ s

(f) $t = 15.0$ s

(i) Elevation (ii) Right side view

Fig. 16. Numerical results based on the hypothesis with deterioration of concrete slabs, corrosion of rebars, and loss of key columns as the main cause.

V. RECENT EVIDENCE AND CONSTRUCTION DEFECTS

Some information and theories were not available at the time this study was conducted, or could not be quantified. Such data has implications for our interpretation of this study.

Engineers who were present on the site during the delayering of the debris attributed the collapse to punching shear of the slabs through the columns. They have also noted that the drawings specified that 25% of the column strip bars were to be run through the column footprints. Such bar concentrations were not found in the remnant columns or the slabs. Discontinuities in reinforcing at the remaining shear wall of the western section were also observed. These hypothetical construction defects could not be quantified for this analysis. But such observations imply that the punching shear capacity could have been greatly diminished by these omissions.

A webinar [7] was conducted on May 25, 2023, by the WJE engineers who summarized new evidence and hypotheses. The factors cited were the mis-location of reinforcing, the obvious punching shear failures at many columns, and the loads added to the pool deck slab. They analyzed the slab-column joints as being under-designed for the shear loads. The WJE analysis identified the same misplacement of column-strip bars outside the column footprint reported by engineers at the site. They also noted that errors in reinforcing placement depth – placing the top bars too low – reduce the effective depth of the slab for punching shear. Most significantly, they found a report of slab/column distress at column L13.1 dated 7 months before the collapse, and another citing slab/planter distress near column K13.1 dated just 22 days before the collapse. The cracks shown in the K13.1 ostensibly show an imminent punching shear failure in the process of degenerating. WJE stated the collapse most likely started with the punching shear failure at these 2 columns.

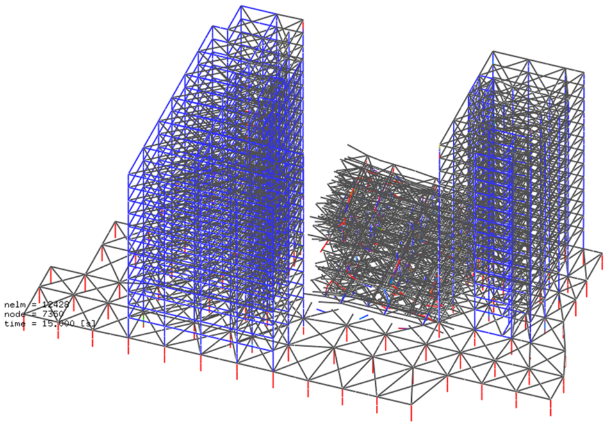

Fig. 17. An isometric view of the numerical result at t = 15.0 s.

The numerical results of this study, such as the lack of collapse behavior in the numerical model until columns were removed or disconnected, tend to confirm the findings offered by WJE. It was difficult to induce a cascading failure in the numerical model, and it never progressed to the eastern section of the building in the model. This numerical model shows that if the building had been nominally constructed according to its design, the loss of several columns would probably not have been enough to progress to sudden failure.

This logic implies another phase is needed for this study. The numerical analysis can be repeated after modeling the reductions in strength due to those construction defects and added loads observed in the field and by the various investigating engineers. The collapse behavior can be compared to the videos and to the debris field to confirm the correlation from reality to model.

VI. Conclusions

In recent years, the progressive collapse of buildings due to the deterioration of structural members has been occurring frequently, posing a significant threat to social assets and human lives. Understanding the collapse mechanism of buildings with deteriorated components or construction defects will enable effective reinforcement of buildings and prevent unexpected collapses. Champlain Towers South, a 13-story beachfront condominium, collapsed at approximately 1:25 a.m. local time on June 24, 2021, in Florida, USA. In this study, we attempted to reproduce the accident based on the investigation data.

First, a 13-story RC building model was analyzed based on the hypotheses published in newspapers. In the case where the extent of pool deck collapse exceeded the key column (Hypothesis 1), neither the final state nor buckling of the key column was confirmed. In the case where the extent of pool deck failure did not exceed the key column (Hypothesis 2), the key column was in the final state, but the entire building did not collapse.

Next, a collapse analysis was conducted based on the hypothesis that removal of key columns was the main cause of the collapse, by constructing a model that considered the pullout of the rebar and the reduction in the bearing capacity of the reinforced concrete. The model confirmed the collapse of the middle section, but no collapse was observed in the eastern section of the building. These results suggest that the pullout of the rebar at the connection joint between the wind-resistant wall and the flat-plate floor, the reduction in bearing capacity of the basement columns, and the removal of key columns were some of the main mechanisms of the collapse of the Florida Condominiums.

There is still room for further study of the phenomenon considering the more recent evidence provided by investigating engineers. Revising the numerical model to reflect construction flaws can provide further confirmation of the hypothetical causes and the observed mechanisms.

Since there are thousands of similar condominium developments in the USA alone, the number of such collapses could increase in the future. Engineers must continue to elucidate the collapse mechanisms of buildings with deteriorated or flawed members. In Florida, and other parts of the world, flat-plate structures have been used because they are economical. New codes and standards mean that many existing buildings must now be re-evaluated, and their collapse mechanisms in worst scenarios, if needed, should be investigated.

Conflict of Interest

The authors declare no conflict of interest.

Author Contributions

Daigoro Isobe: Conceptualization, Methodology, Software, Writing – Original Draft, Writing – reviewing & Editing, Supervision, Project administration, Junnan Zhu: Investigation, Resources, Data curation, Visualization, Janine Pardee: Conceptualization, Writing – reviewing & Editing, Supervision. All authors had approved the final version.

References

[1] KXII News. Caught on camera: Video shows Florida Condo building collapse. [Online]. Available: https://www.kxii.com/2021/06/24/caught-camera-video-shows-florida-condo-building-collapse/

[2] Wikipedia. Surfside condominium collapse. [Online]. Available: https://en.wikipedia.org/wiki/Surfside_condominium_collapse
[3] X. Lu, H. Guan, H. Sun, Y. Li, Z. Zheng, Y. Fei, Z. Yang, and L. Zuo, "A preliminary analysis and discussion of the condominium building collapse in Surfside, Florida, US, June 24, 2021," *Frontiers of Structural and Civil Engineering*, vol. 15, no. 5, pp. 1097–1110, 2021. doi: 10.1007/s11709-021-0766-0.
[4] Morabito Consultants. (October 8, 2018). Champlain Towers South Condominium Structural Field Survey Report. [Online]. Available: https://newsletters.davis-stirling.com/Docs/2018-report.pdf
[5] H. Lew, N. Carino, S. Fattal, and M. Batts, "Investigation of construction failure of harbour cay condominium in Cocoa Beach, Florida," *National Institute of Standards and Technology (NIST)*, Gaithersburg, MD, 1981. doi: 10.6028/NBS.IR.81-2374.
[6] The Washington Post. Interactive investigation into Pool Deck Condo collapse. [Online]. Available: https://www.washingtonpost.com/investigations/interactive/2021/pool-deck-condo-collapse/
[7] M. Fadden and G. Klein, "Webinar: Champlain Towers South Collapse Investigation," Wiss, Janney, Elstner Associates, Inc., May 25, 2023.
[8] D. Isobe, *Progressive Collapse Analysis of Structures: Numerical Codes and Applications*. Elsevier, 2017.
[9] K. M. Lynn and D. Isobe, "Structural collapse analysis of framed structures under impact loads using ASI-Gauss finite element method," *Int. J. Impact Eng.*, vol. 34, pp. 1500–1516, 2007. doi: 10.1016/j.ijimpeng.2006.10.011.
[10] D. Isobe, L. T. T. Thanh, and Z. Sasaki, "Numerical simulations on the collapse behaviors of high-rise towers," *Int. J. Prot. Struct.*, vol. 3, pp. 1-19, 2012. doi: 10.1260/2041-4196.3.1.1.
[11] D. Isobe and K. Itakura, "Collapse scale estimation of a steel-framed building under large-scale fire spread using key element index," *Eng. Struct.*, vol. 289, art. 116324, 2023. doi: 10.1016/j.engstruct.2023.116324.
[12] D. Isobe, W. S. Han, and T. Miyamura, "Verification and validation of a seismic response analysis code for framed structures using the ASI-Gauss technique," *Earthq. Eng. Struct. Dyn.*, vol. 42, pp. 1767–1784, 2013. doi: 10.1002/eqe.1375.
[13] D. Isobe, "An analysis code and a planning tool based on a key element index for controlled explosive demolition," *Int. J. High-Rise Build.*, vol. 3, no. 4, pp. 243–254, 2014.
[14] D. Isobe and R. Jiang, "Explosive demolition planning of building structures using key element index," *J. Build. Eng.*, vol. 59, art. 104935, 2022. doi: 10.1016/j.jobe.2022.104935.
[15] Architectural Institute of Japan. *Design Guidelines for Earthquake Resistant Reinforced Concrete Buildings Based on Inelastic Displacement Concept (Draft)*, 1997.
[16] H. Umemura, *Dynamic Seismic Design for Reinforced Concrete Buildings*. Giho-do, 1973.
[17] T. Kitamura, T. Yoshikawa, and T. Tamakoshi, "Evaluation of anti-seismic performance of road bridge RC pillars using high-strength reinforcement bars," in *Proc. Workshop on Land and Infrastructure Technology*, National Institute for Land and Infrastructure Management, Ministry of Land, Infrastructure and Transport, 2012.
[18] D. Isobe, M. Eguchi, K. Imanishi, and Z. Sasaki, "Verification of blast demolition problems using numerical and experimental approaches," in *Proc. Joint Int. Conf. Computing and Decision Making in Civil and Building Engineering (ICCCBE'06)*, Montreal, Canada, 2006, pp. 446–455.
[19] Town of Surfside. (1979). *Champlain Towers South's Structural Plan. A Development of Toronto Enterprises.* [Online]. Available: https://townofsurfsidefl.gov/departments-services/town-clerk/champlain-towers-public-records-documents (Accessed April 22, 2024).
[20] L. F. M. Sanchez, B. Fournier, M. Jolin, D. Mitchell, and J. Bastien, "Overall assessment of alkali-aggregate reaction (AAR) in concretes presenting different strengths and incorporating a wide range of reactive aggregate types and natures," *Cem. Concr. Res.*, vol. 93, pp. 17–31, 2017. doi: 10.1016/j.cemconres.2016.12.001.